



Extreme flood event reconstruction spanning the last century in the El Bibane Lagoon (southeastern Tunisia): a multi-proxy approach

Aida Affouri^{1,2}, Laurent Dezileau², and Nejib Kallel¹

¹Laboratoire Georessources, Matériaux, Environnements et changements globaux, LR13ES23 (GEOGLOB), Faculté des Sciences de Sfax, Université de Sfax, BP1171, Sfax 3000, Tunisia

²Geosciences Montpellier, CNRS/INSU, UMR5243, Université Montpellier, Montpellier, France

Correspondence to: Aida Affouri (aidaemna@yahoo.fr) and Laurent Dezileau (dezileau@gm.univ-montp2.fr)

Received: 18 March 2016 – Discussion started: 30 March 2016

Revised: 27 April 2017 – Accepted: 3 May 2017 – Published: 19 June 2017

Abstract. Climate models project that rising atmospheric carbon dioxide concentrations will increase the frequency and the severity of some extreme weather events. The flood events represent a major risk for populations and infrastructures settled on coastal lowlands. Recent studies of lagoon sediments have enhanced our knowledge on extreme hydrological events such as palaeo-storms and on their relation with climate change over the last millennium. However, few studies have been undertaken to reconstruct past flood events from lagoon sediments. Here, the past flood activity was investigated using a multi-proxy approach combining sedimentological and geochemical analysis of surface sediments from a southeastern Tunisian catchment in order to trace the origin of sediment deposits in the El Bibane Lagoon. Three sediment sources were identified: marine, fluvial and aeolian. When applying this multi-proxy approach on core BL12-10, recovered from the El Bibane Lagoon, we can see that finer material, a high content of the clay and silt, and a high content of the elemental ratios (Fe / Ca and Ti / Ca) characterise the sedimentological signature of the palaeo-flood levels identified in the lagoonal sequence. For the last century, which is the period covered by the BL12-10 short core, three palaeo-flood events were identified. The age of these flood events have been determined by ²¹⁰Pb and ¹³⁷Cs chronology and give ages of AD 1995 ± 6, 1970 ± 9 and 1945 ± 9. These results show a good temporal correlation with historical flood events recorded in southern Tunisia in the last century (AD 1932, 1969, 1979 and 1995). Our finding suggests that reconstruction of the history of the hydrological extreme

events during the upper Holocene is possible in this location through the use of the sedimentary archives.

1 Introduction

The Mediterranean region has experienced numerous extreme coastal events, such as flood events which caused casualties and economic damages (Lionello et al., 2006). However, the meteorological instrumental records are limited to only a few decades, especially in southern Mediterranean countries. Geological data offer a way to reconstruct the historical records of intense flood events. Deciphering records of extreme precipitation and damaging floods preserved in geologic archives enables society to understand and plan for floods in the future (Parris et al., 2010). The importance of studying trees, river and lake sediments has already been shown for reconstructing extreme flooding events (Baker, 1989; Ely et al., 1993; Brown et al., 2000; Benito et al., 2003; Wolfe et al., 2006; Moreno et al., 2008; Wilhelm et al., 2012; St. George and Nielsen, 2003; Gilli et al., 2013). Few studies have been undertaken to reconstruct past flood events from lagoon sediments (Raji, 2014). Most of the studies were interested in flooding associated with both hurricanes and tsunamis, where overwash deposits are preserved within back-barrier lagoons and salt ponds can provide a means for documenting previous flooding activity (Liu and Fearn, 1993; Donnelly and Woodruff, 2007; Sabatier et al., 2008; Dezileau et al., 2011, 2016; Raji et al., 2015; Degeai et al., 2015). Heavy rain flooding events recorded within these

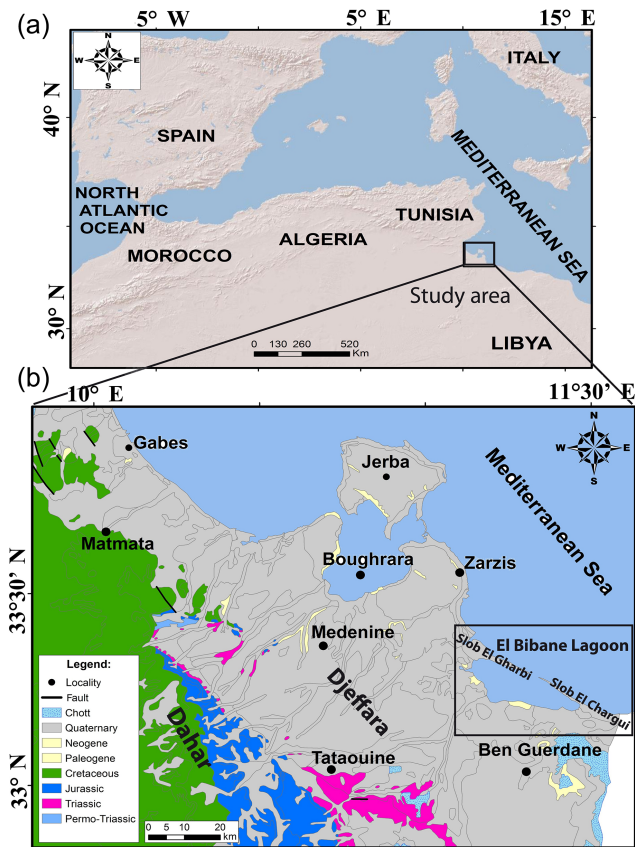


Figure 1. Location of the study area of El Bibane Lagoon, southeastern Tunisia (a), and the geological map of southeastern Tunisia (modified from the geological map of Tunisia, 1 : 500 000, after Ben Haj Ali et al., 1985; b).

lagoon environments are still poorly documented. Moreover, reconstruction of past flood events from sedimentary archives has been poorly studied in Tunisia. Some fluvial archives have been used to reconstruct past flood events in the northern part of Tunisia (Zielhofer et al., 2004; Zielhofer and Faust, 2008) but not in the southern part. In this study we tried to reveal the importance of lagoonal archives to reconstruct past flood activities under a semi-arid environment in the southern part of Tunisia, studying palaeo-floods from high-resolution geochemical and sedimentological analyses. The first aim of this study was to identify the different sediment sources and to retrace the marine, the fluvial and aeolian contributions to the sedimentation in the El Bibane Lagoon. The second aim was to reconstruct flood events from the lagoonal archives during the last century. To reach these objectives, we calibrated the sedimentological and geochemical proxy data with historical flood records.

2 Study site: El Bibane Lagoon and its watershed

Morphologically, southern Tunisia, known as the Tunisian platform, includes two distinguished morpho-tectonic domains (Fig. 1), namely the Djeffara (inner domain) and the Dahar (outer domain). The Djeffara extends over all the coastal plain from Gabès (southeastern Tunisia) to the Libyan borders. It is limited to the west by the Matmata and the Dahar mountains and to the east by the Gulf of Gabès and the Mediterranean Sea. The Dahar belongs to the Saharan platform domain and is constituted by succession sequences ranging in age from the late Permian to the Late Cretaceous (Fig. 1). The lithostratigraphic successions can be summarised as follows: the Early–Middle Triassic sequence in the Dahar Plateau is mainly constituted by continental sandstone, conglomerate and clay, whereas the Late Triassic outcrops exhibit shallow marine carbonate (Busson, 1967). The Jurassic series are represented by a thick Liasic evaporitic sequence, Dogger marine carbonate and Late Jurassic–Neocomian mixed facies with continental predominance (Bouaziz et al., 2002). The Cretaceous series represents a general succession from neritic, lagoonal and continental facies (Mejri et al., 2006). The Late Cretaceous is characterised by thick shallow marine carbonate–marl sequences and covered by sand dunes of the Grand Erg Oriental.

The Mio-Pliocene series represent the substratum of the coastal plain of Djeffara. Jedoui et al. (1998) subdivided these series into two principal facies: (1) the red-coloured clays rich in gypsum and (2) the sands which locally associated with conglomerates and grey clays. The Pleistocene marine deposits of the southeastern Tunisian coastal zone assigned to the “Tyrrhenian” (Marine Isotopic Stage 5e) unconformably overlie the Mio-Pliocene. These deposits form a ridge parallel to the actual coast. They show the superposition of two units described by Jedoui et al. (2002) as the lower “quartz-rich unit” and the upper “carbonate unit” with *Strombus bubonius*.

The study area is focused on the El Bibane Lagoon and its watershed (El Bibane Lagoon: 33° 15′ 01″ N, 11° 15′ 41″ E; Fig. 1). This lagoon, which has an elongated elliptic form (33 × 10 km) and a major WNW–ESE axis, covers an area of about 230 km². It has a maximum water depth of 6 m in the middle part of the basin (Guélorget et al., 1982; Medhioub, 1984). The eastern periphery of the El Bibane Lagoon is partially separated from the Mediterranean Sea (Gulf of Gabès) by two peninsulas, namely El Gharbi (west) and Ech Chargui (east), each of about 12 km long (Medhioub, 1979). These two peninsulas, called *slobs*, are cut at their middle part by nine small islets and channels – the zone of connection with the Mediterranean waters (Medhioub and Perthuisot, 1981). The two *slobs* are represented by emerged Tyrrhenian aeolian littoral dunes and carbonate sand beach (Jedoui, 2000; Jedoui et al., 2002). The El Bibane Lagoon has a microtidal regime where tidal amplitude varies from 0.8 to 1.5 m (Davaud and

Table 1. Geographic location and GPS coordinate of the studied samples.

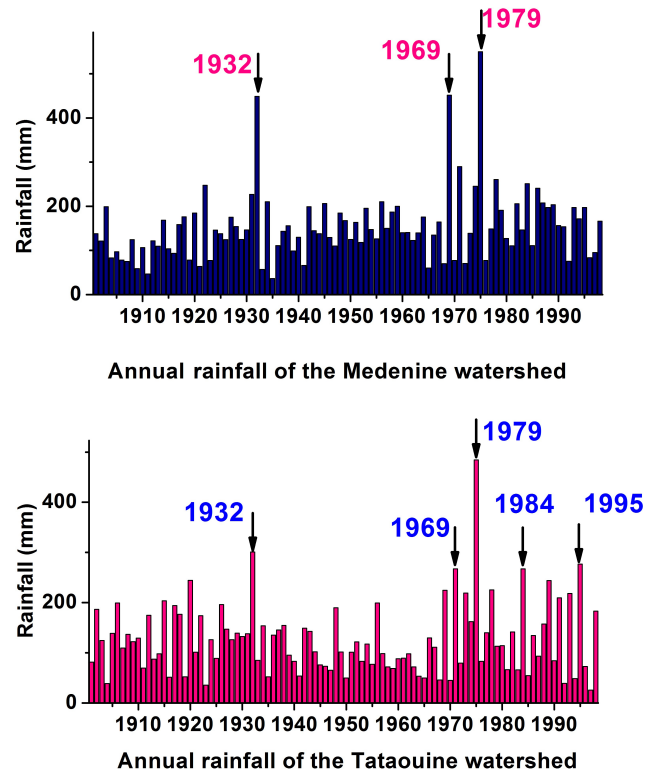
Sample	Locality	GPS coordinates	
		Latitude	Longitude
S1	Beach	33°45′12.4″	10°59′57.9″
S2	Beach	33°35′31.5″	11°04′45.2″
S3	Beach	33°16′39.9″	11°17′39.6″
S4	Lagoon	33°15′38.7″	11°16′40.6″
S5	Lagoon	33°14′0.1″	11°17′.02″
S6	Lagoon	33°13′52.3″	11°06′31.3″
S7	River	33°16′52.3″	11°07′31.3″
S8	River	33°08′03.0″	11°06′51.6″
S9	River	33°03′32.1″	11°02′00.4″
S10	River	33°04′13.6″	10°40′56.0″
S11	River	32°59′23.4″	10°28′12.7″
S12	River	32°55′18.0″	10°24′15.1″
S13	River	32°55′09.7″	10°22′35.3″
S14	River	33°03′38.0″	10°24′05.6″
S15	River	33°09′59.2″	10°21′35.8″
S16	River	33°12′25.37″	10°26′46.78″
S17	Aeolian	33°07′18.9″	10°44′58.6″
S18	Aeolian	32°50′28.4″	10°13′43.7″

Septfontaine, 1995; Sammari et al., 2006). The intertidal flats are flooded and exposed daily at regular intervals during the periodically rising and retreating tide. Supratidal flats are flooded at irregular intervals during spring tides or strong onshore winds (Bouougri and Porada, 2012). The El Bibane Lagoon is relatively unaffected by human activities (Pilkey, 1989; Ounalli, 2001) where it is only exploited by traditional fisheries (Guélorget et al., 1982).

3 Climate and hydrology

The southeastern Tunisia region is characterised by a pre-Saharan and arid to semi-arid climate. The hot season extends beyond the summer (Amari, 1984; Ferchichi, 1996; Hamza, 2003), and the number of sunny days may reach 64.4%. The rainfall is low, with an annual average that does not exceed 200 mm (Hamza, 2003). Furthermore, rainfall fluctuates greatly, with high inter-annual variability and intensity. Most of the rainfall is concentrated within 30 days each year (Genin and Sghaier, 2003), leading to high fluctuations in water discharge. The highest precipitation occurs mainly in October to March while in the summer months there are drought conditions.

The annual precipitations of Medenine and Tataouine stations during the last century were obtained from the Tunisian General Administration of Water Resources (DGRE, 2010, Fig. 2). Five major enhanced precipitation events were recorded from these two stations (i.e. AD 1932, 1969, 1979, 1984 and 1995). These pluvial episodes have induced large flood events in the Fessi River watershed (Poncet, 1970; Bon-

**Figure 2.** Variation in the annual precipitations of the Medenine and Tataouine meteorological stations during the period between 1900 and 2000 (DGRE, 2010).

vallot, 1979; Oueslati, 1999; Boujarra and Ktita, 2009; Fehri, 2014).

4 Materials and methods

4.1 Materials

Eighteen surface sediment samples were collected from the watershed (Jerba, Zarzis, Medenine, Tataouine and Ben Guerdane localities) in order to assess the origin of the material transported into lagoon (Fig. 3). The location of all sampling stations was recorded by GPS (GPSMAP 60, Garmin, Table 1). The main potential sediment sources were sampled in order to characterise their sedimentological and chemical signatures as follows:

- Three samples from the beach area (S1, S2 and S3) representing the marine source.
- Ten samples (S7 to S16) from Fessi River catchment representing the fluvial/river sources.
- Two dune samples (S17 and S18) representing the aeolian component.
- Three surface samples (S4 to S6) from the El Bibane Lagoon have been selected to represent the present-day

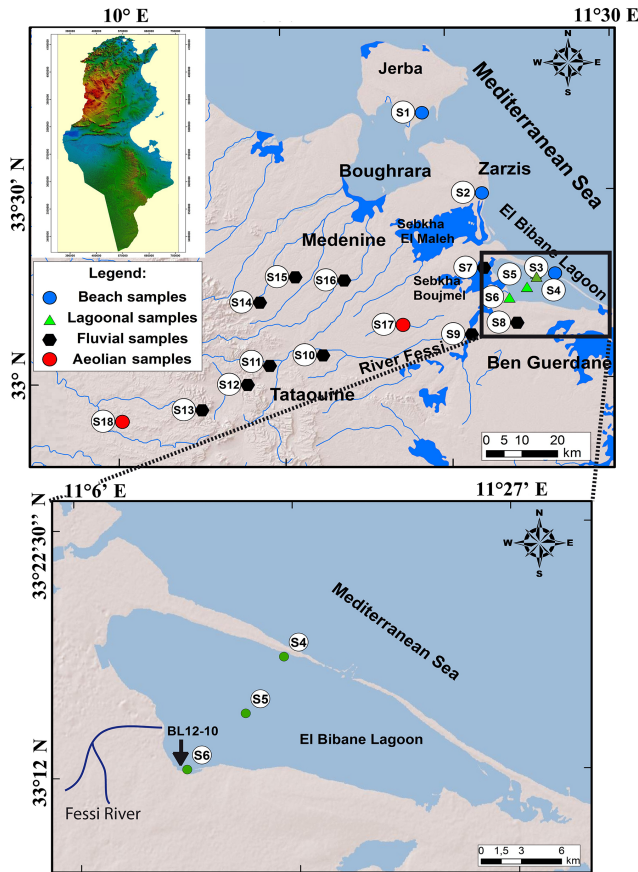


Figure 3. Location of the investigated surface samples from the catchment basin and from the El Bibane Lagoon.

sedimentation. S6, representing the first 3 cm of a lagoon sediment core BL12-10, was used to characterise the surface sediment samples.

Moreover, to reconstruct recent flood events that occurred in the studied area, a short sediment core (BL12-10, 40 cm length; latitude: $33^{\circ}14'58.7''$; longitude: $11^{\circ}10'3.7''$; Fig. 3) was recovered from the El Bibane Lagoon by a hand corer (75 mm diameter PVC tube) in the southern part of the lagoon, at 35 km from the Fessi River delta and 14 km from the connection with the sea.

4.2 Analytical methods

4.2.1 Sedimentological and geochemical analysis

The BL12-10 core was first split, photographed and logged in detail. Elemental geochemical analyses by energy-dispersive X-ray fluorescence (XRF) spectrometry were undertaken with a hand-held Niton XL3t. Measurements were realised on the watershed surface samples and each 2 cm along the BL12-10 core. BL12-10 core and surface samples had been covered with a $4\ \mu\text{m}$ thin Ultralene film to avoid contamination of the XRF measurement unit and the desiccation of the

sediment (Richter et al., 2006). The elemental analyses from XRF measurement were performed in mining-type ModCF proline mode. These data directly show concentrations in ppm or percentage values. This is a semi-quantitative measurement. International powder standards (NIST2702 and NIST2781) were used to assess the analytical error and accuracy of measurement, which are lower than 5 % for Ti, Cr, Fe, Zn and Pb; between 5 and 15 % for Ca, Mn, As, Rb and Sr; and between ca. 15 and 25 % for K and Co.

Laser grain-size analyses were achieved with a Beckmann-Coulter LS13320 particle size analyser (Geosciences Montpellier). Grain-size analyses were performed on surface samples and on the BL12-10 sequence with an average interval of 1 cm. Each sample was sieved through a 1 mm mesh, suspended in deionised water and gently shaken to achieve disaggregation. Ultrasound was used to avoid particles flocculation of sediment in the fluid module of the granulometer. For each sample, a small, homogeneous amount of sediment was mixed in deionised water, then sieved at 1.5 mm diameter before pouring in the fluid module of the particle sizer to obtain an optimal obscuration rate between 7 and 12 % in the Fraunhofer optical cell. The time of background and sample measurement was set to 90 s and sonication was applied during the measurement of the sample in order to improve the dispersion of fine particles in the fluid. Each sample was measured twice and the good repeatability of measurement was verified according to the statistics from the international standard ISO 13320-1.

GRADISTAT program version 4.0 (Blott, 2000) was used for grain-size statistical analysis. The following sample statistics are calculated using the method of moments in Microsoft Visual Basic programming language: mean, mode(s), sorting (standard deviation), skewness and kurtosis. Grain-size parameters are calculated arithmetically, geometrically (in microns) and logarithmically (using the ϕ scale; Krumbein and Pettijohn, 1938). Linear interpolation is also used to calculate statistical parameters by means of the Folk and Ward (1957) graphical method and derive physical descriptions (such as “very coarse sand” and “moderately sorted”).

Finally, the percentage of the granulometric classes <2 , 2–63 and 63–2000 μm , which represent clay, silt and sand fractions, respectively, were calculated.

4.2.2 BL12-10 core dating

Dating of sedimentary layers was carried out using ^{210}Pb and ^{137}Cs methods on a centennial timescale. The ^{137}Cs and $^{210}\text{Pb}_{\text{ex}}$ activities analyses were performed on the fraction $<150\ \mu\text{m}$ by gamma spectrometry using a CANBERRA broad-energy Ge (BEGe) detector (CANBERRA BEGe 3825). The sediment was then finely crushed after drying, transferred into small tubes (diameter 14 mm) and stored for more than 3 weeks to ensure equilibrium between ^{226}Ra and ^{222}Rn . Generally, counting times of 24 to 48 h were required to reach a statistical error of less than 10 % for $^{210}\text{Pb}_{\text{ex}}$ in

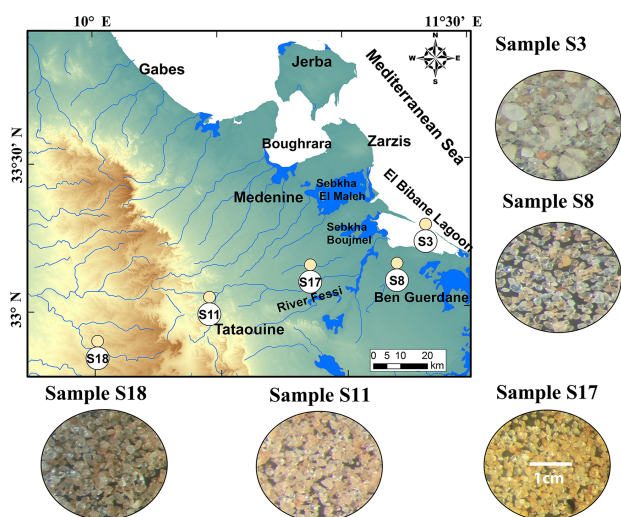


Figure 4. Microtextural photos under binocular microscope observation of five representative samples from the catchment basin of El Bibane Lagoon. S3: marine sample; S8 and S11: Fessi River samples; S17 and S18: dunes samples (diameter of the photos: 3 cm; $G \times 6.5$).

the deepest samples and for the 1963 ^{137}Cs peak. Activities of ^{210}Pb were determined by integrating the area of the 46.5 keV photo-peak. ^{226}Ra activities were determined from the average of values derived from the 186.2 keV peak of ^{226}Ra and the peaks of its progeny in secular equilibrium with ^{214}Pb (295 and 352 keV) and ^{214}Bi (609 keV). In each sample, the $(^{210}\text{Pb}\text{-unsupported})_{\text{ex}}$ activities were calculated by subtracting the $(^{226}\text{Ra}\text{-supported})$ activity from the total (^{210}Pb) activity. We then used the constant flux/constant sedimentation (CFCS) model and the decrease in $^{210}\text{Pb}_{\text{ex}}$ to calculate the sedimentation rate (Goldberg, 1963). The uncertainty in the sedimentation rate obtained by this method was derived from the standard error of the linear regression of the CFCS model.

^{137}Cs was studied on core BL12-10 in order to assess sediment accumulation rates and chronology of the first 30 cm of the core. ^{137}Cs ($t_{1/2} = 0.1$ year) is an anthropogenic radionuclide. It entered the environment in response to atmospheric nuclear tests from AD 1954 to 1980 that induced global fallout events (the first year of atmospheric releases was AD 1953, whereas the maximum atmospheric production was reached in AD 1963). ^{137}Cs depth profiles have been extensively used in various environments to assess sediment accumulation rates (Nittrouer et al., 1984; He and Walling, 1996; Radakovitch et al., 1999; Frignani et al., 2004).

4.2.3 Statistical analyses

Statistical methods were applied to complete and refine the analysis. Principal component analysis (PCA) is widely used statistical techniques in environmental geochemistry. This

multivariate approaches is used to reduce the large number of variable that result from XRF analysis. PCA was applied to elements in order to distinguish the different sediment sources of surface sediments and link them to the geochemical processes or proprieties. In the present work, the dataset contains 18 samples, each of which includes concentration of eight elements (Ca, Sr, Fe, K, Al, Ti, Si and Zr). Data are presented in the form of elemental concentration (eight variables). In this study, a statistical analysis was performed using STATITCF (1987), which is based on variables and it is suitable for identifying the associations of variables with a set of observations. A representation quality of the parameters (positions in the factorial plane) was then performed.

5 Results

5.1 Surface sediments

5.1.1 Sediment description: grain size and morphology

Grain-size analysis and binocular microscope observation of the surface sediment samples have permitted us to characterise three groups of sediments as follows, depending on the environmental setting: marine, fluvial and aeolian sources (Figs. 4 and 5). The first group encompasses sediment samples (S1, S2 and S3) collected along the coastal zone from Jerba to Zarzis beaches and the lido of El Bibane Lagoon. In this marine area, surface sediments are composed of a mixture of coarse sub-rounded quartz grains, mollusc shells and foraminifera (Fig. 4). The grain-size analyses (Table 2) of samples S1 and S2 show unimodal distributions of 169 and 203 μm , respectively, indicating moderately sorted fine sand sediments (Folk, 1954; Folk and Ward, 1957; Fig. 5). Sample S3 is muddy sand, i.e. very coarse silty to coarse sand sediment with unimodal distribution of 518 μm .

The second group of samples (S7, S8, S9, S10, S11, S12, S13, S14, S15 and S16) came from the El Bibane Delta and the Fessi River. It is assigned as the fluvial source. Binocular microscope observations of the samples reveal reddish-brown heterogeneous particles composed mainly of shiny angular to sub angular quartz grains. Some grains display a rust colour from iron oxide (Fig. 4). Figure 5 displays that the fluvial source has a unimodal to multimodal distribution with two or three modes. In order to obtain the best resolution in the identification of the fluvial source, we choose to use the sediment samples which were collected only along the Fessi River: S9, S10, S12 and S13. These surface sediment samples show a decrease in the mean grain size from upstream to downstream of the Fessi River watershed (Fig. 6). The decrease in the mean grain size could be explained by a strong change in the topographic slope around Tataouine (located at approximately 85 km from the lagoon). Here, the coarser material is deposited and the finer material is transported further by the river. These finer sediments are deposited in the low plain of the river and in the El Bibane Lagoon. Therefore, we

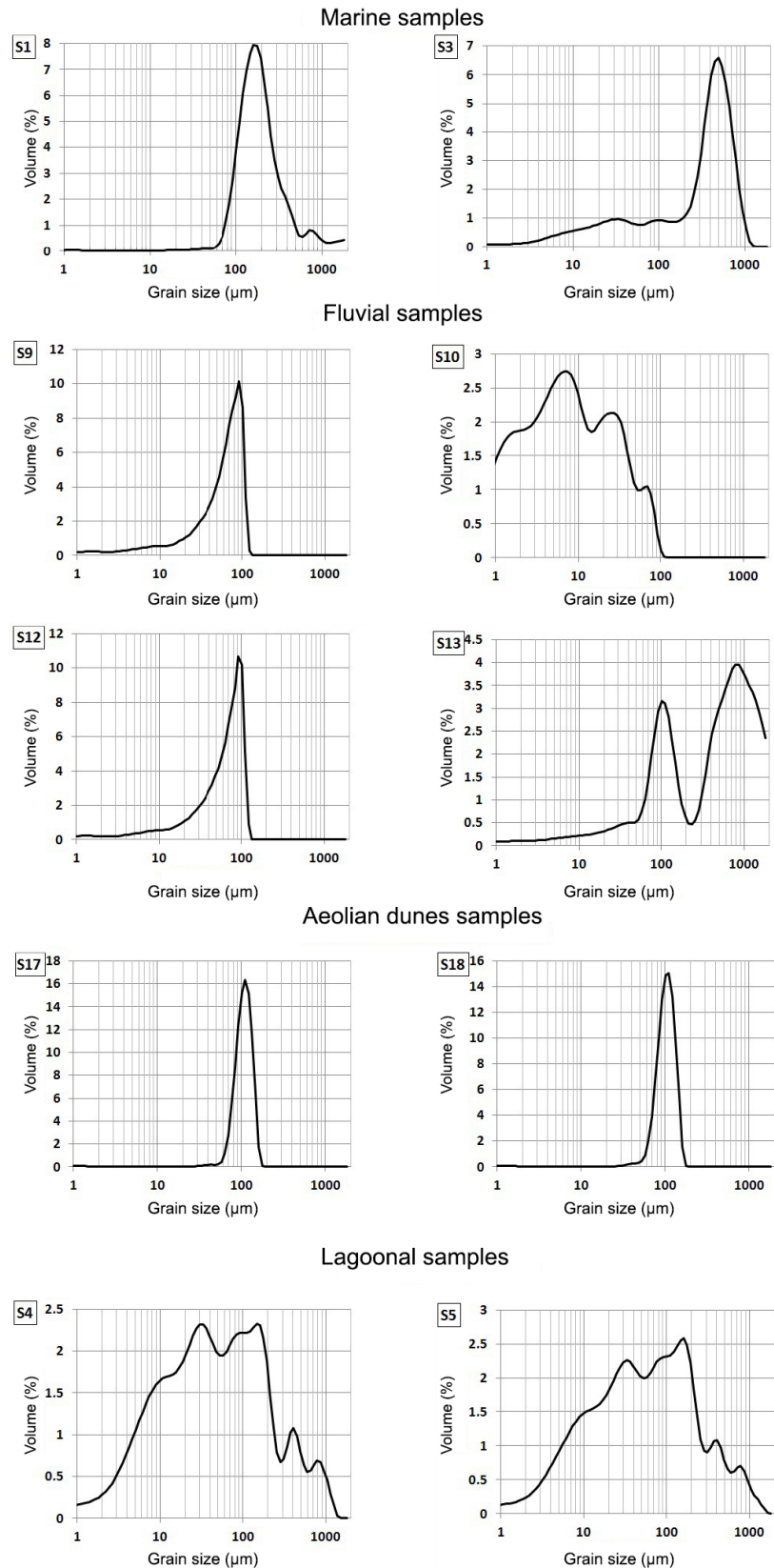
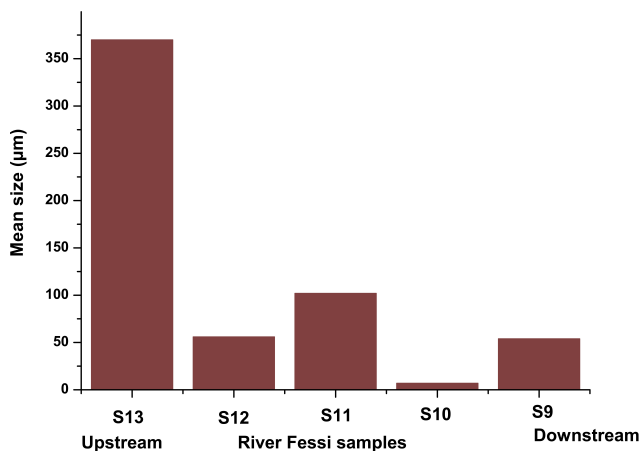


Figure 5. Particle size distributions (< 2000 μm) of representative samples from the catchment basin and the El Bibane Lagoon.

Table 2. Grain-size statistical analysis of surface samples from the watershed of the El Bibane Lagoon.

Sample name	Sampling locality	Sample type	Textural group	Sediment name
S1	Beach	Unimodal, moderately sorted	Sand	Moderately sorted fine sand
S2		Unimodal, moderately sorted	Sand	Moderately sorted fine sand
S3	Surface sediments El Bibane Lagoon	Unimodal, very poorly sorted	Muddy sand	Very coarse silty coarse sand
S4		Polymodal, very poorly sorted	Sandy mud	Very fine sandy, very coarse silt
S5		Unimodal, moderately sorted	Muddy sand	Very coarse silty, fine sand
S6		Bimodal, poorly sorted	Muddy sand	Very coarse silty, very fine sand
S9	Fessi River	Unimodal, poorly sorted	Muddy sand	Very coarse silty, very fine sand
S10		Trimodal, poorly sorted	Mud	Fine silt
S11		Unimodal, well sorted	Sand	Well-sorted, very fine sand
S12	Sand dune	Unimodal, poorly sorted	Muddy sand	Very coarse silty, very fine sand
S13		Bimodal, poorly sorted	Muddy sand	Very coarse silty, coarse sand
S17		Unimodal, very well sorted	Sand	Very well-sorted, very fine sand
S18		Unimodal, well sorted	Sand	Well-sorted, very fine sand

Folk and Ward method (μm)							
Sample name	Mean	Sorting	Skewness	Kurtosis	Mode 1 (μm)	Mode 2 (μm)	Mode 3 (μm)
S1	196.20	1.79	0.23	1.31	169.10		
S2	249.10	1.81	0.18	1.11	203.70		
S3	204.20	4.23	-0.66	1.02	517.80		
S4	43.46	4.68	-0.03	0.93	154.00	31.54	96.60
S5	112.50	1.81	-0.22	1.20	116.40		
S6	80.39	3.15	-0.24	1.70	106.00	429.70	
S9	54.69	2.24	-0.57	1.49	96.60		
S10	7.13	3.89	0.00	0.84	7.09	26.17	73.02
S11	102.50	1.34	-0.24	1.22	116.40		
S12	56.17	2.25	-0.57	1.42	96.60		
S13	370.90	3.90	-0.41	0.88	825.40	106.00	
S17	110.50	1.26	-0.13	1.01	116.40		
S18	106.40	1.29	-0.13	1.03	116.40		

**Figure 6.** Distribution of the mean size of the samples collected in the Fessi River.

suggest that S9 and S10 (collected between Tataouine and the lagoon) characterise the fluvial component in the lagoon. The grain-size distribution for S9 is unimodal with a mean grain size around $96\ \mu\text{m}$, indicating a moderately sorted muddy sand. The corresponding size range very coarse silty/very fine sand. Sample S10 is fine silt with trimodal distribution in 7, 26 and $73\ \mu\text{m}$, and poorly sorted mud sediment type. These characteristics will serve to identify the fluvial source into the lagoon.

The third group consists of two samples (S17 and S18) recovered in the aeolian sand dunes of southern Tunisia. These samples are composed of homogeneous dark-yellow sand with angular grains; some of them are coated by iron oxide (Fig. 4). Unimodal distribution in $116\ \mu\text{m}$ (Table 2) characterises the aeolian samples S17 and S18. These samples are well (S18) to very well sorted (S17) and correspond to very fine sand. The characteristics of this group will serve to identify the aeolian sand dune source.

The El Bibane Lagoon surface sediment samples S4, S5 and S6 were characterised by multimodal grain-size distribution (Table 2, Fig. 5). The grain-size distribution of sample

Table 3. XRF analysis results of the major and trace elements in studied samples.

Sample name	Locality	Zr (ppm)	Sr (ppm)	Ca (%)	Fe (%)	Ti (%)	K (%)	Al (%)	Si (%)
S1	Beach	113	1497	14.67	0.00	0.03	0.14	0.00	9.71
S2	Beach	41	1548	14.51	0.00	0.01	0.10	0.00	6.85
S3	Beach	24	899	13.36	0.00	0.01	0.10	0.00	8.38
S4	Lagoon	133	1035	17.35	0.75	0.13	0.74	0.40	15.00
S5	Lagoon	85	747	9.00	0.47	0.10	0.47	0.18	8.70
S6	Lagoon	203	418	7.90	0.27	0.07	0.56	0.69	12.00
S7	River	134	358	17.35	0.75	0.13	1.10	2.08	15.00
S8	River	488	90	9.00	0.53	0.10	0.81	2.60	8.70
S9	River	178	97	7.90	0.98	0.07	1.13	2.76	12.00
S10	River	235	105	7.30	1.52	0.21	1.36	4.20	26.16
S11	River	704	92	6.00	0.59	0.16	0.56	2.20	26.93
S12	River	275	173	7.37	1.22	0.21	1.12	3.60	27.43
S13	River	391	123	7.35	1.28	0.18	0.93	2.60	27.13
S14	River	458	186	7.16	0.79	0.20	0.87	2.70	26.18
S15	River	350	102	3.95	0.59	0.17	0.77	2.40	29.08
S16	River	263	73	3.22	0.62	0.11	0.74	1.80	25.62
S17	Aeolian	473	52	0.80	0.40	0.10	0.75	2.50	33.38
S18	Aeolian	357	54	0.81	0.38	0.12	0.74	2.40	33.09

S4 shows very poorly sorted sandy mud with trimodal distribution at 154, 96 and 31 μm , which indicates a very fine sand/very coarse silt. Sample S5 is very coarse silty/very fine sand sediment, with a bimodal distribution in 106 and 429 μm , poorly sorted muddy sand. Sample S6 is unimodal, with a mode of 116 μm . It is a moderately sorted very coarse silty/fine sand sediment with a muddy sand texture (Folk, 1954; Folk and Ward, 1957).

5.2 Distribution of major and trace elements

The spatial distribution of major and trace elements in surface sediments collected in the El Bibane Lagoon and in all the area mainly along the Fessi River is displayed in Fig. 7.

Iron (Fe) shows its highest percentages in the Fessi River samples (0.53–1.52 %). Lower values characterise the aeolian dunes (0.38–0.4 %), whereas this element is totally absent in marine sediments (Table 3). The same distribution pattern is also observed for Ti, K and Al. The highest contents of these elements in the Fessi River samples contrast with the lowest ones retrieved in the marine surface sediment. Aeolian dunes are characterised by intermediate values. These four elements will thus be used as indicators of terrigenous input of material to the lagoon.

Calcium (Ca) and strontium (Sr) in the sediment are usually associated with the carbonate fraction, which can be either of allochthonous or autochthonous origin. In the sediments, carbonates are mainly of biogenic origin. In fact, due to its compatible ionic radius, Sr can replace Ca in calcite, but remains, however, as a trace element (Fig. 7). Nevertheless, both elements show the same distribution pattern. Marine surface sediments are associated with the highest values (Ca \approx 14.7 %; Sr \approx 1548 ppm), whereas the lowest values

and thus the lowest calcite contents are retrieved in dune samples (Ca \approx 0.8 %; Sr \approx 52 ppm). Intermediate concentrations are associated with the Fessi River catchment (Ca \approx 7 %; Sr \approx 150 ppm) (Table 3).

Silicon (Si) and Zircon (Zr) follow a similar spatial distribution pattern (Fig. 7). Higher contents of these elements are observed in the river catchment samples (Si \approx 20 %; Zr \approx 300 ppm) and in the aeolian dune samples (Si \approx 33 %; Zr \approx 400 ppm), whereas marine sediments show generally lower contents (Si \approx 10 %; Zr \approx 41 ppm; Table 3).

5.3 Principal component analysis (PCA)

We used PCA to identify the main factors controlling the chemical composition of the catchment and El Bibane Lagoon surface sediments and to identify different groups of common origin and process. Application of PCA varimax rotation has permitted to identify two components that explained 83 % of the total variance (Fig. 8). Factor 1 accounts for 64.46 % of total variance. It is characterised by high positive loadings for Fe, Ti, K, and Al, which indicates the dominance of alumino-silicates minerals in surface sediments (Spagnoli et al., 2008; Plewa et al., 2012). These elements are prevailing in the river surface samples and their granulometric distributions shows that their grain sizes are in the range of clay and silt. Zr and Si display a moderately positive loading in factor 1 and are high in the aeolian surface sediments. Zr and Si are associated with silicates originating either from adjacent desert areas by erosion or from western Saharan dunes by storms.

Factor 2 accounts for 17.73 % of the total variance (Fig. 8). It shows positive loading for Ca, Sr, Fe and K, whereas Ti, Al, Zr and Si have negative loadings. Ca is high in the ma-

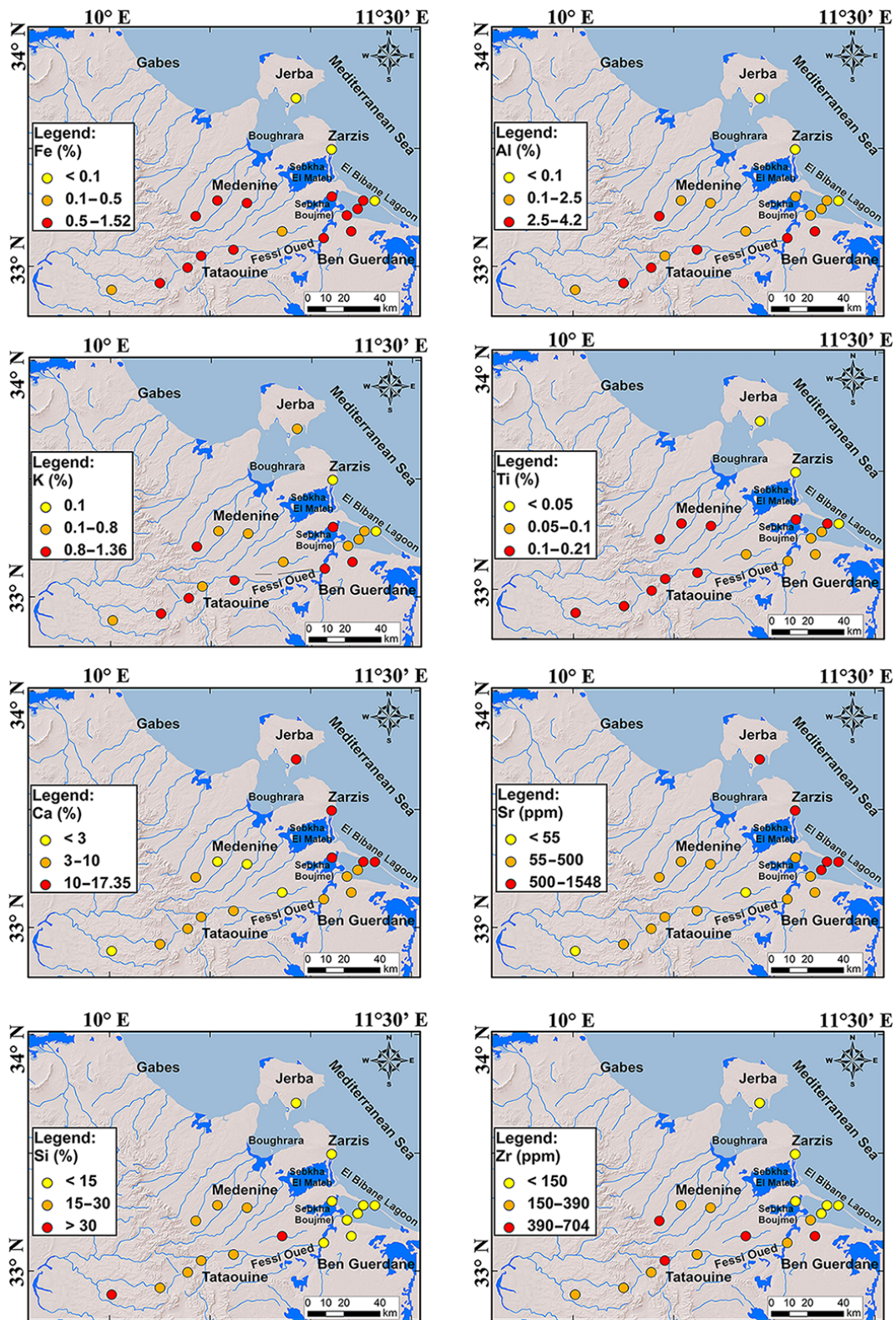


Figure 7. Distribution map of major and trace elements in surface sediments from the catchment basin and the El Bibane Lagoon.

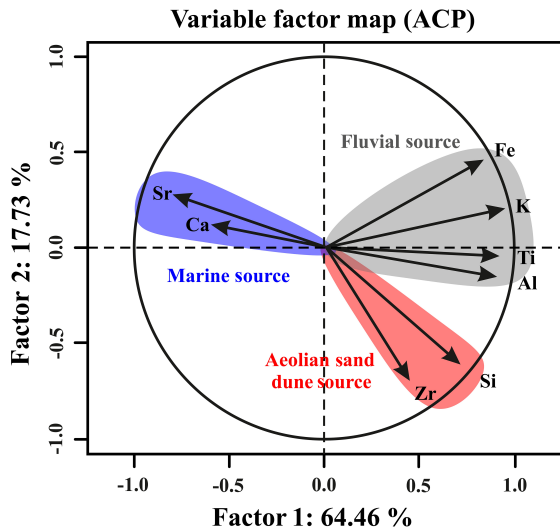


Figure 8. Principal component analysis (PCA) loadings plot of major and trace element concentrations displaying the three main sources: marine, fluvial and aeolian sand dune.

rine samples. The high percentage of Ca in these samples is related to both the significant presence of biogenic material and also probably the precipitation of authigenic carbonate. These results corroborate the marine origin of these sediments as revealed by the binocular microscope observations mainly due to the existence of shell debris and confirmed by the grain-size distributions. Therefore, we suggested that the first component agreed with the fine fraction of the sediment, which is mainly composed of various types of clay minerals, usually abundant in surface sediments (De Lazari et al., 2004). On the other hand, factor 2 (Fig. 8) provides a better definition of the relatively carbonate fraction of the sediments. Consequently, these two factors differentiated carbonates from both sand and clay sediments. This method allowed us to label elements of terrigenous source (Fe, Ti, K and Al) from those from in situ marine origin (Ca and Sr). These proxies will be used to reconstruct past flood and storm events with the help of sedimentary archives.

5.4 El Bibane Lagoon: main sediment sources

Geochemical parameters as well as grain-size data are useful indicators for the detection of significant facies changes in the stratigraphical record (Vött et al., 2002; Zhu and Weindorf, 2009). Statistical analyses of geochemical data have permitted to characterise the different sediment sources around the El Bibane Lagoon. Ca, Ti and Fe elements have been chosen in order to recognise the contribution of these sources to the surface sediments of the Lagoon. Ca displays its highest abundances in the marine area and is lower in sand dunes and river samples. By contrast, Ti characterises the continental source (see Sect. 5.1.2) and shows low contents in marine samples. On the other hand, Fe is present as a

Table 4. Activities of radionuclides ^{210}Pb , ^{137}Cs and ^{226}Ra along core BL12-10.

Depth (cm)	^{226}Ra (dpm g $^{-1}$)	^{210}Pb (mbq g $^{-1}$)	^{137}Cs (mbq g $^{-1}$)
0	0.586 ± 0.007	14.584 ± 1.157	0.507 ± 0.081
3	0.556 ± 0.009	11.486 ± 1.202	0.655 ± 0.098
6	0.592 ± 0.008	12.142 ± 0.924	0.872 ± 0.085
9	0.574 ± 0.008	11.066 ± 1.221	0.908 ± 0.096
12	0.596 ± 0.008	6.729 ± 1.048	0.883 ± 0.080
15	0.598 ± 0.003	7.466 ± 1.175	1.782 ± 0.104
18	0.582 ± 0.008	8.877 ± 1.103	2.375 ± 0.115
21	0.592 ± 0.005	6.110 ± 1.005	1.060 ± 0.084
40	0.659 ± 0.011	1.058 ± 1.476	0.365 ± 0.101

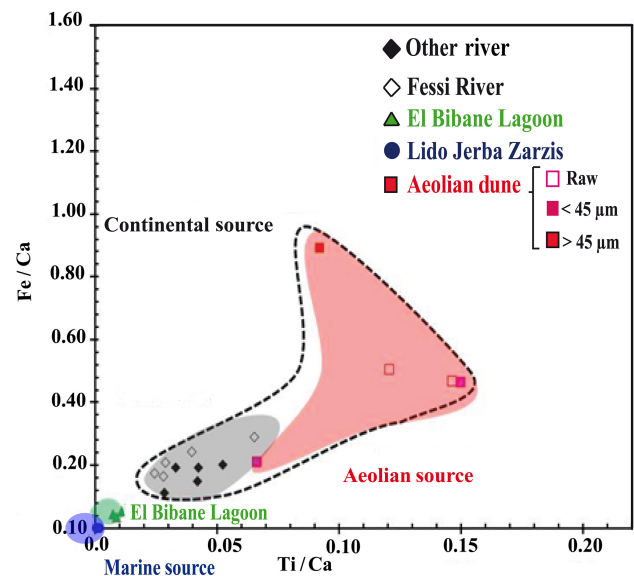
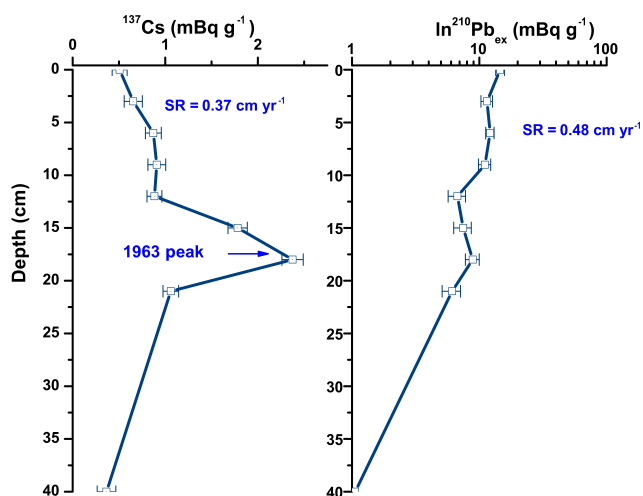


Figure 9. Distribution of the investigated surface samples from the watershed and the El Bibane Lagoon on a cross-plot of Fe / Ca versus Ti / Ca.

maximum in the river samples and as a trace element in marine samples. Taking into account this geographic distribution, Fe / Ca as well as Ti / Ca ratios values would be higher in the continental supply (fluvial and aeolian samples) and lower in the marine source. High Fe / Ca values due to high iron content may also reflect dominating subaerial weathering and oxidation. The Fe / Ca and Ti / Ca ratio values and the position on a Fe / Ca vs. Ti / Ca diagram (Fig. 9) of El Bibane Lagoon surface sediments (samples S4, S5 and S6) are intermediate between the marine and fluvial source. Accordingly, higher Fe / Ca and Ti / Ca ratios in the lagoon sediments would be a signal of more sediment contribution from fluvial source to the lagoon during flooding. As shown before, the Fessi River sediments were characterised by fine material with a grain size which does not exceed $63 \mu\text{m}$ (case of S9 and S10; see Sect. 5.1.1).

Table 5. Grain-size statistical analysis along core BL12-10.

Depth (cm)	Sample name	Sample type	Textural group	Sediment name
1	BL12-10-1	Bimodal, poorly sorted	Muddy sand	Very coarse silty, very fine sand
2	BL12-10-2	Trimodal, very poorly sorted	Muddy sand	Very coarse silty, very fine sand
3	BL12-10-3	Trimodal, poorly sorted	Muddy sand	Very coarse silty, very fine sand
4	BL12-10-4	Trimodal, very poorly sorted	Muddy sand	Very coarse silty, very fine sand
5	BL12-10-5	Trimodal, poorly sorted	Muddy sand	Very coarse silty, very fine sand
6	BL12-10-6	Trimodal, poorly sorted	Muddy sand	Very coarse silty, very fine sand
7	BL12-10-7	Trimodal, poorly sorted	Muddy sand	Very coarse silty, very fine sand
8	BL12-10-8	Bimodal, poorly sorted	Muddy sand	Very coarse silty, very fine sand
9	BL12-10-9	Bimodal, poorly sorted	Muddy sand	Very coarse silty very fine sand
10	BL12-10-10	Trimodal, poorly sorted	Muddy sand	Very coarse silty, very fine sand
11	BL12-10-11	Trimodal, poorly sorted	Muddy sand	Very coarse silty, very fine sand
12	BL12-10-12	Trimodal, very poorly sorted	Muddy sand	Very coarse silty, very fine sand
13	BL12-10-13	Trimodal, poorly sorted	Muddy sand	Very coarse silty, very fine sand
14	BL12-10-14	Trimodal, very poorly sorted	Muddy sand	Very coarse silty, very fine sand
15	BL12-10-15	Trimodal, poorly sorted	Muddy sand	Very coarse silty, very fine sand
16	BL12-10-16	Trimodal, very poorly sorted	Muddy sand	Very coarse silty, very fine sand
17	BL12-10-17	Trimodal, very poorly sorted	Muddy sand	Very coarse silty, very fine sand
18	BL12-10-18	Trimodal, very poorly sorted	Muddy sand	Very coarse silty, very fine sand
19	BL12-10-19	Trimodal, very poorly sorted	Muddy sand	Very coarse silty, very fine sand
20	BL12-10-20	Bimodal, poorly sorted	Muddy sand	Very coarse silty, very fine sand
21	BL12-10-21	Bimodal, poorly sorted	Muddy sand	Very coarse silty, very fine sand
22	BL12-10-22	Trimodal, poorly sorted	Muddy sand	Very coarse silty, very fine sand
23	BL12-10-23	Trimodal, poorly sorted	Muddy sand	Very coarse silty, very fine sand
24	BL12-10-24	Bimodal, poorly sorted	Muddy sand	Very coarse silty, very fine sand
25	BL12-10-25	Trimodal, poorly sorted	Muddy sand	Very coarse silty, very fine sand
26	BL12-10-26	Trimodal, poorly sorted	Muddy sand	Very coarse silty, very fine sand
27	BL12-10-27	Trimodal, very poorly sorted	Muddy sand	Very coarse silty, very fine sand
28	BL12-10-28	Trimodal, very poorly sorted	Muddy sand	Very coarse silty, very fine sand
29	BL12-10-29	Trimodal, poorly sorted	Muddy sand	Very coarse silty, very fine sand
30	BL12-10-30	Bimodal, poorly sorted	Muddy sand	Very coarse silty, very fine sand

**Figure 10.** $^{210}\text{Pb}_{\text{ex}}$ and ^{137}Cs activity–depth profiles along core BL12-10. SR: sedimentation rate (cm yr^{-1}).

5.5 Core BL12-10

5.5.1 ^{210}Pb and ^{137}Cs dating

The measured ^{210}Pb values in the uppermost 30 cm of the BL12-10 core range from 14.5 to 0.1 mBq g^{-1} (Table 4). In general, the down-core distribution of $^{210}\text{Pb}_{\text{ex}}$ values follows a relatively exponential decrease with depth and the CFCS sedimentation model was applied. The calculated sedimentation rate (SR) is about 0.48 cm yr^{-1} . The down-core ^{137}Cs activity profile (Fig. 10) shows a maximum at 18 cm depth (Table 4). We attributed this maximum to the period of maximum radionuclide fallout in the Northern Hemisphere associated with the peak of atomic weapons testing in 1963. The ^{137}Cs -derived SR (0.37 cm yr^{-1}) is lower than that of the ^{210}Pb (Fig. 10). The difference between the two methods could be explained by a change in the accumulation rate between the beginning and the last part of the 20th century.

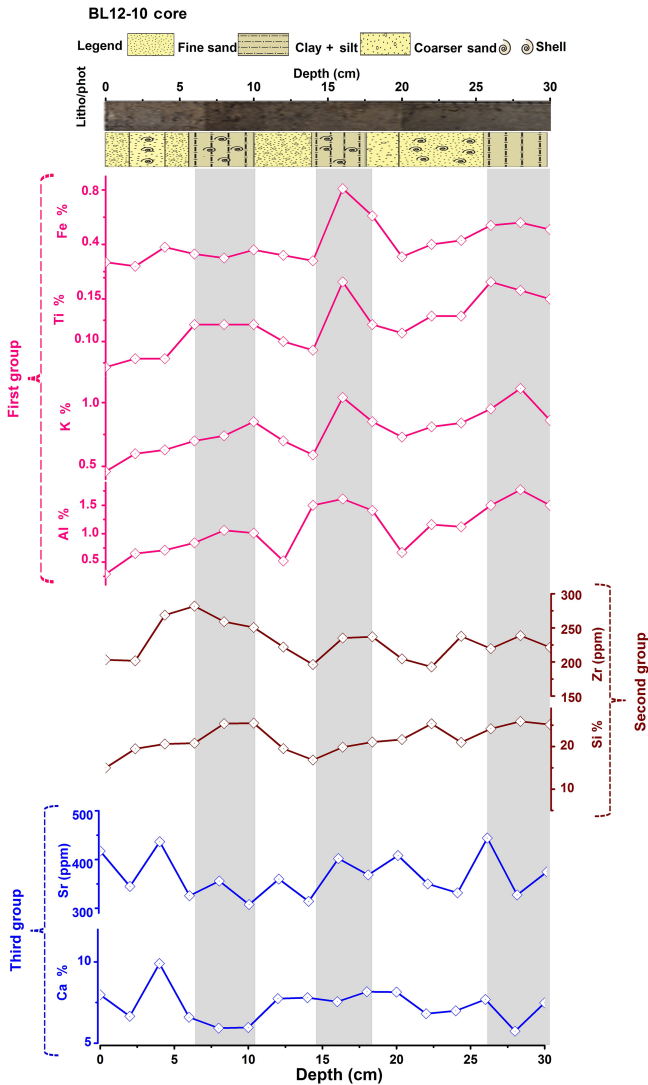


Figure 11. Records of eight geochemical elements (expressed in percentage or ppm) versus depth in core BL12-10.

5.5.2 Sedimentary and geochemistry

The sediment sequence from El Bibane Lagoon presented in this study come from core BL12-10 recovered in the nearest part of the delta of Fessi River in May 2012. This study proposes the preliminary analyses performed on the first 30 cm only, although the whole BL12-10 core length is 90 cm. The BL12-10 core is composed of coarse-grained layers of siliciclastic sand and shell fragments inter-bedded with organic-rich, dark-grey, fine-grained sediment (mud) of clay and silt (Fig. 11). These coarse layers are interbedded with three mud layers from 6 to 10, 14 to 18 and 26 to 30 cm core depth (Fig. 11). The thickest fine-grained layers are typically composed of clay and silt sediments. Core BL12-10 is dominated by the bimodal and trimodal grain-size distributions. These distributions were labelled as very coarse silty to very fine

sand, poorly to very poorly sorted, fine skewed with leptokurtic distribution (Table 5). Down-core profiles of heavy and light elements through the depth also delineate the different units distinguished by sedimentological analysis (Fig. 11). Based on their profiles, the first group composed by Fe, Ti, K and Al exhibit similar variations, concentration values are mainly high in fine-grained intervals and are low in coarse-grained intervals. These high values are probably due to high inputs from the Fessi River. The Si and Zr which characterised the second group display a different behaviour than the first group (Fig. 11). These two elements are high in the fine sandy intervals. This probably suggests that their highest values are related to aeolian inputs in the lagoon. The Ca and Sr characterising the third group show a reverse distribution pattern in comparison to the first group, with higher values in the coarse-grained intervals and lower values in the fine-grained intervals (Fig. 11). Single element concentrations may be too sensitive to dilution effects to allow reliable reconstructions of terrestrial climate, elemental ratios often better reflect the origin of the sedimentary material. The measured elemental ratios Fe / Ca and Ti / Ca will be used to reconstruct past flood events (Fig. 9). A higher Fe / Ca and Ti / Ca ratio in the lagoon sediments would be a signal of more sediment contribution from the Fessi River during flooding.

6 Discussion

6.1 Palaeo-flood reconstructions

In order to identify the palaeo-flood events of the El Bibane Lagoon, we applied these previously discussed proxies to BL12-10 core samples. The BL12-10 core shows three mud layers (clay and silt mixture) preserved in the core, which seem to be flood layers, i.e. coming from fluvial incursions during intense flood events. Multiproxy analysis on these mud layers shows that they are characterised by a high content of clay+silt, as well as high Fe / Ca and Ti / Ca elemental ratios, which represent the sedimentological signature of the Fessi River. The combination of geochemical and grain-size data suggest that the BL12-10 core deposits had registered three flood events, namely FL1, FL2 and FL3 (Fig. 12). These flood deposits have a thickness of 5, 4 and 2.5 cm respectively.

Our palaeo-flood reconstruction has been compared with historical rainfall data of Tataouine and Medenine (DGRE, 2000; Fehri, 2014). A good correlation is observed between instrumental rainfall records and past flood events recorded in the El Bibane Lagoon. Based on our age model, FL1 would have occurred around AD 1995 \pm 6 years (Fig. 12). This sediment deposit could correspond to the 1995 flood event recorded in hydrological data (Fehri, 2014) and which affected the entire Tataouine region. This flood reached a maximum discharge of 1200 m³ s⁻¹ due to a heavy precipitation event over 24 h (Boujarra and Ktita, 2009). These events

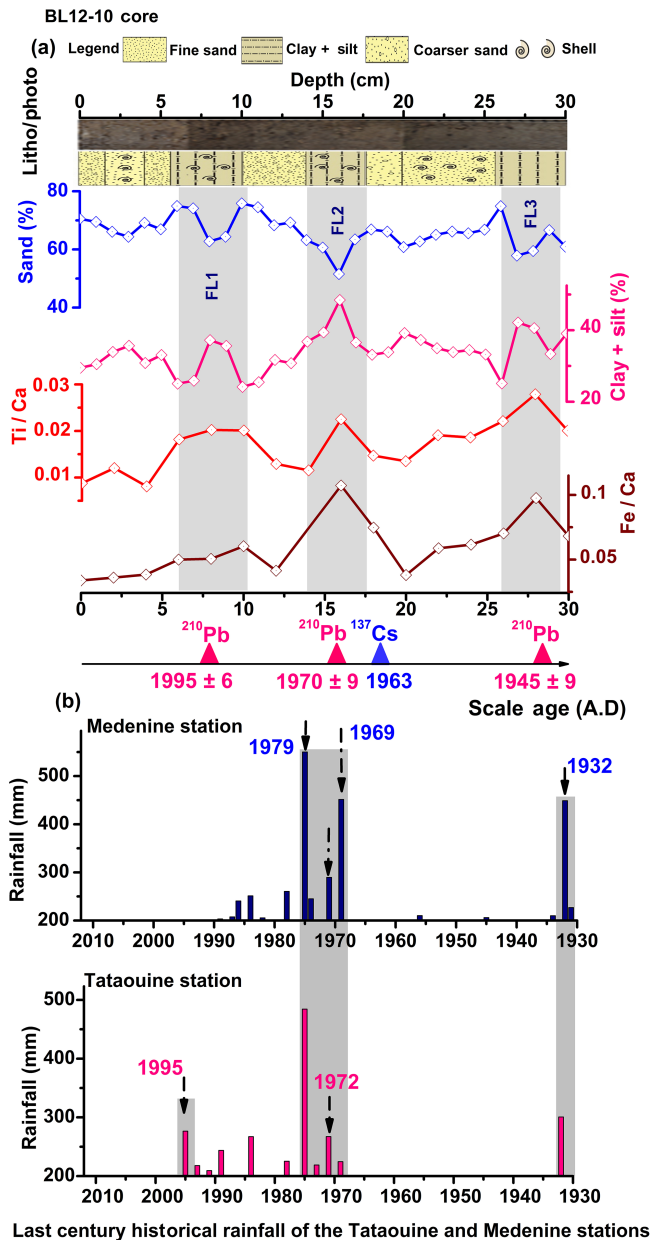


Figure 12. (a) Palaeo-flood records in the sedimentary archive of core BL12-10 based on elemental ratios of Fe / Ca and Ti / Ca and grain-size analysis (clay + silt; fraction <math> < 63 \mu\text{m}</math>). Triangles indicate the age control obtained using ^{210}Pb and ^{137}Cs along the core. Coloured areas display the three periods of floods recorded in the core (FL1, FL2 and FL3). (b) The observed rainfall record since 1932 in Medenine and Tataouine stations is also shown.

caused heavy losses in human lives and agricultural goods (Boujarra and Ktita, 2009). Using the same approach, FL2 would have occurred around AD 1970 ± 9 years, i.e. between AD 1965 and 1980 (Fig. 12). Between these dates, two historical extreme flood events are known (AD 1969 and 1979) and one flood event of lower magnitude (AD 1972). The 1969 flood event is characterised by a heavy precipitation

event (400 to 600 mm) over 24 to 48 h (Pias and Stuckmann, 1970; Kallel et al., 1972; Boujarra and Ktita, 2009). The 1979 flood event is characterised by a heavy precipitation during 4 days (Bonvallet, 1979). Only one horizon corresponds to these events in the BL12-10 core. Consequently, we assume that this unique flood deposit registers a period during which these three high-precipitation events occurred (i.e. AD 1969, 1972 and 1979). The activity of ^{210}Pb in this flood deposit is not disturbed; it is homogeneous (Fig. 10). For this reason we assume that no significant erosion happened in the lagoon during this period. During these heavy precipitation events, most of the sedimentary material was deposited in the flood-plain and the lagoon and probably transported to the Mediterranean Sea through the passes. The sedimentation rate corresponding to these events is not very high. The thickness of the sediment layer associated with these flood events is low, i.e. about 5 cm. The grain size and geochemical values of this flood deposit are rather homogeneous. This homogeneity is probably linked to the action of weak bottom currents within the El Bibane Lagoon. Finally, since these three extreme flood events are very close together in time (1969–1979) and the sedimentation rate is low, they are recorded as only one sedimentary deposit (FL2) in our archive. The third flood event FL3 was dated at AD 1945 ± 9 (Fig. 12). It could be associated with the 1932 flood event (Fehri, 2014). This event was characterised by a flash flood event with a precipitation event of 449 mm in a few days. Bonvallet (1979) demonstrated that this event presents a similar characteristic to that of 1979.

The El Bibane flood record shows temporal correspondence of flood layers to historical heavy precipitation events. Considering the historical data, we can assume that the FL3 flood deposit corresponds to the AD 1932 flood. The FL2 flood deposit is associated with the AD 1969, 1972 and 1979 flood events. The FL1 flood deposit could be associated with the AD 1995 flood event (Fig. 12). In this lagoonal environment, one flood deposit is not always associated with a single event but sometimes with two or three events, especially when heavy precipitation events are close together in time (i.e. FL2 flood deposit). Moreover, these data demonstrate that finer material with a high content of mud (clay + silt) and high ratios of Fe / Ca and Ti / Ca are associated with flood events in the lagoonal sequence. The association of these proxies in the sedimentary sequence of the El Bibane Lagoon can therefore be used to reconstruct flood activities in southeastern Tunisia.

6.2 The El Bibane Lagoon: a key region for palaeohydrological reconstructions

Lagoon records shows that such coastal environments are good study areas to record past climatic and environmental changes, as well as extreme sea events. These fields of research were successfully applied in the western North Atlantic (Donnelly and Woodruff, 2007), northwestern Florida

(Liu and Fearn, 2000; Lane et al., 2011; Das et al., 2013), the northeastern United States (Parris et al., 2010), the central Pacific (Toomey et al., 2013), southern Japan (Woodruff et al., 2009), western Australia (Nott, 2011), northeastern New Zealand (Page et al., 2010), northern Europe (Sorrel et al., 2012), or the western Mediterranean (Dezileau et al., 2011, 2016; Sabatier et al., 2012; Raji et al., 2015; Degeai et al., 2015). Such studies are still scarce in southern Tunisia, despite the importance of these topics in Mediterranean coastal areas. The El Bibane Lagoon is different from the other studied lagoons because it cannot record coastal overwash events. Such particularity is linked to the morphology of barriers that separate this lagoon from the open sea. These barriers consist of two narrow fossil carbonate consolidated peninsula formed during the last interglacial period and reaching 10 m elevation (Medhioub, 1979; Jedoui, 2000). Thus, they cannot not be over-washed during extreme sea events. However, we have demonstrated from this study that this lagoon could record past flood events during exceptional heavy precipitation episodes that punctuated the recent meteorological and climatic history of Tunisia and North Africa. Trambly et al. (2013) analysed the influence of large-scale atmospheric circulation, including the North Atlantic Oscillation (NAO), Mediterranean Oscillation (MO), El Niño–Southern Oscillation (ENSO) and Western Mediterranean Oscillation (WEMO) on precipitations and extreme events in 22 stations located in Algeria, Morocco and Tunisia for the last 50 years. Although some spatial patterns for the different precipitation indices have been identified over Maghreb countries the southern part of Tunisia was only represented by one meteorological station (Gabès). This clearly avoid to identify an homogeneous climatic region, there is a need to include more stations with longer record length. El Bibane Lagoon palaeo-flood record can be of great importance to better understand the physical mechanism responsible for the changes in the frequency and/or the intensity of extreme events in the southern part of Tunisia. It will be interesting to study the natural variability of past flood events in this semi-arid environment through contrasting climatic periods (cold and warm periods). Upcoming investigations on long core sediments could clarify the relationship between large-scale atmospheric circulation reconstructions and the major flood periods (Affouri et al., 2017a). Additionally, such studies could be a crucial tool to evaluate the role of Mediterranean palaeo-climate on the development and growth of human society.

7 Conclusions

This study focuses on the sedimentological and geochemical characterisation of the main surface sediment sources of El Bibane Lagoon (southeast Tunisia) and its watershed in order to identify the specific signature of palaeo-flood events recorded in the sedimentary core archives. We used principal component analysis (PCA) to identify the main factors

controlling the chemical composition of the catchment and El Bibane Lagoon surface sediments and to discriminate between the sources of detrital inputs into the lagoon. Three sediment sources were identified: marine, fluvial and aeolian. Our results display that El Bibane Lagoon surface sediment characteristics are situated between marine and river sources. The application of this multi-proxy analysis on the BL12-10 core shows that finer material, high content of mud (clay + silt), and high elemental ratios (Fe / Ca and Ti / Ca) typify the sedimentological signature of flood events in the lagoonal sequence. The BL12-10 age model based on ^{210}Pb and ^{137}Cs activity profiles have allowed us to identify three periods of past flood events dated at $\text{AD } 1995 \pm 6$, 1970 ± 9 and 1945 ± 9 . The good agreement between our estimated ages and the historical flood events suggests that sedimentological and geochemical data of lagoon sediment cores could be used to reconstruct palaeo-flood history in southeastern Tunisia in arid and semi-arid environments during the upper Holocene.

Data availability. Please find my data in: <https://doi.pangaea.de/10.1594/PANGAEA.876044> (Affouri et al., 2017b).

Competing interests. The authors declare that they have no conflict of interest.

Acknowledgements. Our thanks go to M. Ouaja, P. Blanchemache and J. P. Degai for their help in the field. We also thank Y. Jedoui and G. Siani for their fruitful suggestions in the discussions. This study is funded by the projects FP7-IRSES MEDYNA 2014-2017, MISTRALS PALEOMEX and PHC-UTIQUE no. 14G1002. We are particularly grateful to the editor, Nathalie Combourieu-Nebout, for comments. We thank Maria-Angella Bassetti, MCF-HDR assistant professor at the University of Perpignan, France, and the anonymous reviewers for their helpful comments and their criticism, which led to a considerable improvement of the manuscript.

Edited by: N. Combourieu Nebout

Reviewed by: six anonymous referees

References

- Affouri, A., Dezileau, L., and Kallel, N.: Late Holocene paleoclimatic reconstruction inferred from EL Bibane lagoon (Southeast of Tunisia), in preparation, 2017a.
- Affouri, A., Dezileau, L., and Kallel, N.: Grain size and geochemical analysis in the El Bibane Lagoon and the Fessi River watershed (Southeast of Tunisia), <https://doi.org/10.1594/PANGAEA.876044>, 2017b.
- Amari, A.: Contribution à la connaissance hydrologique et sédimentologique de la plateforme des îles Kerkennah Thèse de 3ème cycle, Faculté des Sciences de Tunis, Tunis, 1984.

- Baker, V. R.: Magnitude and frequency of paleofloods, in: *Floods: Hydrological, Sedimentological, and Geomorphological Implications*, edited by: Beven, K. and Carling, P., Wiley, Chichester, 171–183, 1989.
- Ben Haj Ali, M., Jedoui, Y., Dali, T., Ben Salem, H., and Memmi, L.: La Carte géologique à l'échelle 1/500 000 de la Tunisie. Serv. Géol. Tunisie, 1985.
- Benito, G., Díez-Herrero, A., and Fernández de Villalta, M.: Magnitude and Frequency of Flooding in the Tagus Basin (Central Spain) over the Last Millenium', *Clim. Change*, 58, 171–192, 2003.
- Blott, S. J.: Gradistat version 4.0 – A Grain Size Distribution and Statistics Package for the Analysis of unconsolidated sediments by Sieving or Laser Granulometer, Surface Processes and Modern Environments Research Group, Department of Geology, Royal Holloway, University of London, Egham, Surrey TW20 0EX, 2000.
- Bonvallet, J.: Comportement des ouvrages de petite hydraulique dans la région de Médenine (Tunisie du Sud) au cours des pluies exceptionnelles de mars 1979, les Cahiers de l'O.R.S.T.O.M, Série Sciences Humaines XVI, 3, 233–249, 1979.
- Bouaziz, S., Barrier, E., Souissi, M., Turki, M. M., and Zouari, H.: Tectonic evolution of the northern African margin in Tunisia from paleostress data and sedimentary record, *Tectonophysics* 357, 227–253, 2002.
- Boujarra, A. and Kïta, A.: Les facteurs de l'amplification de l'inondation de la ville de Tataouine le 24 septembre 1995 (SUD EST TUNISIEN), Risques naturelles en Méditerranée occidentale, 195–206, 2009.
- Bouougri, E. H. and Porada, H.: Wind-induced mat deformation structures in recent tidal flats and sabkhas of SE-Tunisia and their significance for environmental interpretation of fossil structures, *Sediment. Geol.*, 263–264, 56–66, 2012.
- Busson, G.: Le mésozoïque saharien Ière partie: l'Extrême Sud tunisien. Centre National de la Recherche Scientifique, Paris, *Géologie*, 8, 204 pp., 1967.
- Brown, S. L., Bierman, P. R., Lini, A., and Southon, J.: 10 000 yr records of extreme hydrologic events, *Geology*, 28, 335–338, 2000.
- Das, O., Wang, Y., Donoghue, J., Xu, X., Coor, J., Elsner, J., and Xu, Y.: Reconstruction of paleostorm and paleoenvironment history using geochemical proxies archived in the sediments of two coastal lakes in NW Florida, *Quaternary Sci. Rev.*, 68, 142–153, 2013.
- Davaud, E. and Septfontaine, M.: Post-mortem onshore transportation of epiphytic foraminifera: recent example from the Tunisian coastline, *J. Sediment. Res.*, 65, 136–142, 1995.
- Degeai, J. P., Devillers, B., Dézileau, L., Oueslati, H., and Bony, G.: Major storm periods and climate forcing in the Western Mediterranean during the Late Holocene, *Quaternary Sci. Rev.*, 129, 37–56, 2015.
- Dezileau, L., Sabatier, P., Blanchemanche, P., Joly, B., Swingedouw, D., Cassou, C., Castaings, J., Martinez, P., and Von Grafenstein, U.: Intense storm activity during the Little Ice Age on the French Mediterranean coast, *Palaeogeogr. Palaeocl.*, 299, 289–297, 2011.
- Dezileau, L., Pérez-Ruzafa, A., Blanchemanche, P., Degeai, J.-P., Raji, O., Martinez, P., Marcos, C., and Von Grafenstein, U.: Extreme storms during the last 6500 years from lagoonal sedimentary archives in the Mar Menor (SE Spain), *Clim. Past*, 12, 1389–1400, <https://doi.org/10.5194/cp-12-1389-2016>, 2016.
- De Lazzari, A., Rampazzo, G., and Pavoni, B.: Geochemistry of sediments in the Northern and Central Adriatic Sea, *Estuarine, Coast. Shelf Sci.* 59, 429–440, 2004.
- Direction Générale des Ressources en Eaux (DGRE): *Annuaire hydrométéorologiques 1976 2010*, Ministère de l'Agriculture, l'Environnement et les ressources en eau, Tunisie, 2010.
- Donnelly, J. P. and Woodruff, J. D.: Intense hurricane activity over the past 5000 years controlled by El Nino and the West African monsoon, *Nature*, 447, 465–468, 2007.
- Ely, L. L., Enzel, Y., Baker, V. R., and Cayan, D. R.: A 5000-year record of extreme flood and climatechange in the southwestern United States, *Science*, 262, 410–412, 1993.
- Fehri, N.: L'aggravation des risques d'inondation en Tunisie : éléments de réflexion. *Physio-Géo, Géographie, physique et environnement*, 8, 149–175, 2014.
- Ferchichi, A.: Etude climatique en Tunisie présaharienne : proposition d'un nouvel indice de subdivision climatique des étages méditerranéens aride et saharien, *Medit (italy)*, 3/96, 46–53, 1996.
- Folk, R. L.: The distinction between grain size and mineral composition in sedimentary rock nomenclature, *J. Geol.*, 62, 344–359, 1954.
- Folk, R. L. and Ward, W. C.: Brazos river bar: A study in the significance of grain size parameters, *J. Sediment. Petrol.*, 27, 3–26, 1957.
- Frignani, M., Sorgente, D., Langone, L., Albertazzi, S., and Ravaioli, M.: Behaviour of Chernobyl radiocesium in sediments of the Adriatic Sea off the Po River delta and the Emilia-Romagna coast, *J. Environ. Radioactivity*, 71, 299–312, 2004.
- Genin, D. and Sghaier, M.: Pratiques et usages des ressources, techniques de lutte et devenir des populations rurales, Rapport scientifique final de synthèse, IRA, IRD (Projet Jeffara), 20, 2003.
- Gilli, A., Anselmetti, F. S., Glur, L., and Wirth, S. B.: Lake Sediments as Archives of Recurrence Rates and Intensities of Past Flood Events, Dating Torrential Processes on Fans and Cones, *Adv. Glob. Change Res.*, 47, 225–242, https://doi.org/10.1007/978-94-007-4336-6_15, 2013.
- Goldberg, E.: Geochronology with lead-210, International Atomic Energy Agency, 121–131, 1963.
- Guélorget, O., Frisoni, G. F., and Perthuisot, J. P.: Contribution à l'étude biologique de la Bahiret el Biban: lagune du Sud-Est Tunisien, *Mémoires de la Société Géologique de France*, 144 pp., 173–186, 1982.
- Hamza, A.: Le statut du phytoplancton dans le golfe de Gabès. Thèse de Doctorat, Université de Sfax, 298, 2003.
- He, Q. and Walling, D. E.: Use of fallout Pb-210 measurements to investigate longer-term rates and patterns of overbank sediment deposition on the floodplains of lowland rivers, *Earth Surf. Proc. Land.*, 21, 141–154, 1996.
- Jedoui, Y.: Sédimentologie et géochronologie des dépôts littoraux quaternaires: reconstitution des variations des paléoclimats et du niveau marin dans le Sud-Est tunisien, Thèse d'Etat es. Sciences, Fac. Sc. Tunis, Université de Tunis El Manar, 338 pp., 2000.
- Jedoui, Y., Kallel, N., Fontugne, M., Ben Ismail, M. H., M'Rabet, A., and Montacer, M.: A relative sea-level stand in the middle Holocene of southeastern Tunisia: *Marine Geology*, 147, 123–130, 1998.

- Jedoui, Y., Davaud, E., Ben Ismaïl, H., and Reyss, J. L.: Analyse sédimentologique des dépôts marins pléistocènes du Sud-Est tunisien: mise en évidence de deux périodes de haut niveau marin pendant le sous-stade isotopique marin 5e (Eémien, Tyrrhénien), *Bulletin de la Société Géologique de France*, 173, 63–72, 2002.
- Kallel, R., Colombani, J., Eoche duval, J. M.: Les précipitations et les crues exceptionnelles de l'automne 1969 en Tunisie, publication de la division des ressources en eau, Ressources en eau de Tunisie, 1972.
- Krumbein, W. C. and Pettijohn, F. J.: *Manual of Sedimentary Petrography*. Appleton-Century-Crofts, New York, 1938.
- Lane, P., Donnelly, J. P., Woodruff, J. D., and Hawkes, A. D.: A decadal-resolved paleohurricane record archived in the late Holocene sediments of a Florida sinkhole, *Mar. Geol.*, 287, 14–30, 2011.
- Lionello, P., Bhend, J., Buzzi, A., Della-Marta, P., Krichak, S., Jansa, A., Maheras, P., Sanna, A., Trigo, I., and Trigo, R.: Cyclones in the Mediterranean region: climatology and effects on the environment, *Develop. Earth Environ. Sci.*, 4, 325–372, 2006.
- Liu, K. B. and Fearn, M. L.: Lake-sediment record of late Holocene hurricane activities from coastal Alabama, *Geology*, 21, 793–796, 1993.
- Liu, K.-B. and Fearn, M. L.: Reconstruction of Prehistoric Landfall Frequencies of Catastrophic Hurricanes in Northwestern Florida from Lake Sediment Records, *Quaternary Res.*, 54, 238–245, 2000.
- Medhioub, K.: La Bahiret El Bibane, Etude géochimique et sédimentologique d'une lagune du Sud-Est tunisien, Travail du laboratoire de Géologie, Presse de l'école Normale Supérieure, Paris, 13, 150 pp., 1979.
- Medhioub, K.: Etude géochimique et sédimentologique du complexe paralique de la dépression de ben Guirden: Bahira el Biban, Sabkha bou J'Mel et Sabkha el Medina, Thèse Doctorat es-Sciences, Ecole Normale Supérieure, Paris, 400 pp., 1984.
- Medhioub, K. and Perthuisot, J. P.: The influence of peripheral sabkhas on the geochemistry and sedimentology of a Tunisian lagoon: Bahiret el Biban, *Sedimentology*, 28, 679–688, 1981.
- Mejri, F., Burolet, P. F., and Ben Ferjani, A.: Petroleum geology of Tunisia: A renewed synthesis, *Memoir ETAP*, 22, 233 pp., 2006.
- Moreno, A., Valero-Garcés, B., Gonzales-Sampériz, P., and Rico, M.: Flood response to rainfall variability during the last 2000 years inferred from the Taravilla Lake record (Central Iberian Range, Spain), *J. Paleolimnol.*, 40, 943–961, 2008.
- Nittrouer, C. A., DeMaster, D. J., Kuehl, S. A., McKee, B. A., and Thorbjarnarson, K. W.: Some questions and answers about the accumulation of fine-grained sediments in continental margin environments, *Geo-Mar. Lett.*, 4, 211–213, 1984–1985.
- Nott, J.: A 6000 year tropical cyclone record from Western Australia, *Quaternary Sci. Rev.*, 30, 713–722, 2011.
- Ounalli, A.: Projet de dessalement d'eau de mer à El Bibane, *Desalination*, 137, 293–296, 2001.
- Oueslati, A.: Les inondations en Tunisie, Publication à compte d'auteur, 206 pp., 1999.
- Page, M. J., Trustrum, N. A., Orpin, A. R., Carter, L., Gomez, B., Cochran, U. A., Mildenhall, D. C., Rogers, K. M., Brackley, H. L., Palmer, A. S., and Northcote, L.: Storm frequency and magnitude in response to Holocene climate variability, Lake Tutira, North-Eastern New Zealand, *Mar. Geol.*, 270, 30–44, 2010.
- Parris, A. S., Bierman, P. R., Noren, A. J., Prins, M. A., and Lini, A.: Holocene paleostorms identified by particle size signatures in lake sediments from the northeastern United States, *J. Paleolimnol.*, 43, 29–49, 2010.
- Poncet, J.: La catastrophe climatique de l'automne 1969 en Tunisie, *Annales de Géographie*, 79, 581–595, 1970.
- Pias, J. and Stuckmann, G.: Les inondations de septembre-octobre 1969 en Tunisie, Partie 2 Etude morphologique, UNESCO, Paris, 1970.
- Pilkey, O. H.: A thumbnail method for beach communities: estimation of long-term beach replenishment requirements, *Shore and Beach*, 23–31 July, 1989.
- Plewa, K., Meggers, H., Kuhlmann, H., Freudenthal, T., Zabel, M., and Kasten, S.: Geochemical distribution patterns as indicators for productivity and terrigenous input off NW Africa, *Deep-Sea Res. Pt. I*, 66, 51–66, 2012.
- Raji, O.: Evénements extrêmes du passé et paleo-environnements: reconstruction à partir des archives sédimentaires de la lagune Nador, Maroc, Thèse de Doctorat, Université Mohammed V de Rabat, 2014.
- Raji, O., Dezileau, L., Von Grafenstein, U., Niazi, S., Snoussi, M., and Martinez, P.: Extreme sea events during the last millennium in the northeast of Morocco, *Nat. Hazards Earth Syst. Sci.*, 15, 203–211, <https://doi.org/10.5194/nhess-15-203-2015>, 2015.
- Radakovitch, O., Charmasson, S., Arnaud, M., and Bouisset, P.: 210Pb and caesium accumulation in the Rhône delta sediments, *Estuar. Coast. Shelf Sci.*, 48, 77–92, 1999.
- Richter, T. O., Van der Gaast, S., Koster, B., Vaars, A., Gieles, R., de Stigter, H. C., De Haas, H., and Van Weering, T. C. E.: The Avaatech XRF Core Scanner: technical description and applications to NE Atlantic sediments, in: *Techniques in Sediment Core Analysis*, edited by: Rothwell, R. G., Geological Society of London, Special Publications, 39–50, 2006.
- Sabatier, P., Dezileau, L., Condomines, M., Briquieu, L., Colin, C., Bouchette, F., Le Duff, M., and Blanchemanche, P.: Reconstruction of paleostorm events in a coastal lagoon (Hérault, South of France), *Mar. Geol.*, 251, 224–232, 2008.
- Sabatier, P., Dezileau, L., Colin, C., Briquieu, L., Bouchette, F., Martinez, P., and Von Grafenstein, U.: 7000 years of paleostorm activity in the NW Mediterranean Sea in response to Holocene climate events, *Quaternary Res.*, 77, 1–11, 2012.
- Sammari, C., Koutitonsky, V. G., and Moussa, M.: Sea level variability and tidal resonance in the Gulf of Gabes, Tunisia, *Cont. Shelf Res.*, 26, 338–350, 2006.
- Sorrel, P., Debret, M., Billeaud, I., Jaccard, S. L., McManus, J. F., and Tessier, B.: Persistent non-solar forcing of Holocene storm dynamics in coastal sedimentary archives, *Nat. Geosci.*, 5, 892–896, 2012.
- Spagnoli, F., Bartholinia, G., Dinelli, E., and Giordano, P.: Geochemistry and particle size of surface sediments of Gulf of Manfredonia (Southern Adriatic Sea), *Estuarine, Coast. Shelf Sci.*, 80, 21–30, 2008.
- St. George, S. and Nielson, E.: Paleoflood records for the Red River, Manitoba, Canada, derived from anatomical tree-ring signatures, *Holocene*, 13, 547–555, 2003.
- Tramblay, Y., El Adlouni, S., and Servat, E.: Trends and variability in extreme precipitation indices over Maghreb countries, *Nat. Hazards Earth Syst. Sci.*, 13, 3235–3248, <https://doi.org/10.5194/nhess-13-3235-2013>, 2013.

- Toomey, M. R., Donnelly, J. P., and Woodruff, J. D.: Reconstructing mid-late Holocene cyclone variability in the Central Pacific using sedimentary records from Tahaa, French Polynesia, *Quaternary Sci. Rev.*, 77, 181–189, 2013.
- Vött, A., Handl, M. and Brückner, H.: Rekonstruktion holozäner Umweltbedingungen in Akarnanien (Nordwestgriechenland) mittels Diskriminanzanalyse von geochemischen Daten, *Geologica et Palaeontologica*, 36, 123–147, 2002.
- Wilhelm, B., Arnaud, F., Sabatier, P., Crouzet, Ch., Elodie, B., Eric, Ch., Jean-Robert, D., Frederic, G., Emmanuel, M., Jean-Louis, R., Kazuyo, T., Edouard, B., and Jean-Jacques, D.: 1400 years of extreme precipitation patterns over the Mediterranean French Alps and possible forcing mechanisms, *Quaternary Res.*, 78, 1–12, 2012.
- Wolfe, B. B., Hall, R. I., Last, W. M., Edwards, T. W. D., English, M. C., Karst-Riddoch, T. L., Paterson, A., and Palmmini, R.: Reconstruction of multi-century flood histories from oxbow lake sediments, Peace-Athabasca Delta, Canada, *Hydrol. Process*, 20, 4131–4153, 2006.
- Woodruff, J. D., Donnelly, J. P., and Okusu, A.: Exploring typhoon variability over the mid-to-late Holocene: evidence of extreme coastal flooding from Kamikoshiki, Japan, *Quaternary Sci. Rev.*, 28, 1774–1785, 2009.
- Zielhofer, C., Faust, D., Baena, R., Diaz del Olmo, F., Kadereit, A., Moldenhauer, K.-M., and Porras, A.: Centennial-scale late Pleistocene to mid-Holocene synthetic profile of the Medjerda floodplain (Northern Tunisia), *Holocene*, 14, 851–861, 2004.
- Zielhofer, C. and Faust, D.: Mid- and Late Holocene fluvial chronology of Tunisia, *Quaternary Science Reviews*, 27, 580–588, 2008.
- Zhu, Y. and Weindorf, D.: Determination of soil calcium using field portable X-ray fluorescence, *Soil Sci.*, 174, 151–155, 2009.